JOURNAL OF THERMOPHYSICS AND HEAT TRANSFER
Vol. 9, No. 3, July–September 1995

Technical Notes

TECHNICAL NOTES are short manuscripts describing new developments or important results of a preliminary nature. These Notes cannot exceed 6 manuscript pages and 3 figures; a page of text may be substituted for a figure and vice versa. After informal review by the editors, they may be published within a few months of the date of receipt. Style requirements are the same as for regular contributions (see inside back cover).

Preliminary Temperature Stabilization of Space Telescopes

Sergey V. Tikhonov* and Alexander V. Boytsev†
Heat Transfer Laboratory,
St. Petersburg 195112, Russia

Introduction

DURING on-orbit operation, a spacecraft is subjected to significant variations of external thermal conditions due to the intensive cooling by radiation losses to space and by the solar heating of separate sections of a spacecraft surface. Due to the variable orientation of the spacecraft relative to the sun, the solar conditions are also variable. These variations are of particular significance for optical systems whose elements require a near uniform temperature distribution.

In space telescope designs, significant attention is payed to the control of the temperatures required for the front assembly elements. This is of special importance for telescopes operating at cryogenic temperatures.[1-3] Temperature control is achieved through a careful selection of temperature control coatings, sunshade system optimization, and installation of additional sunshadows. The effectiveness of these techniques is corroborated by the successful Infrared Astronomical Satellite (IRAS) flight.[1] The necessity of the front assembly temperature stabilization applies to optical devices that operate at temperatures near 300 K, particularly for variable orientations relative to the sun.[4]

Front assembly temperature control is closely connected with the design principles and parameters of the thermal control system. The smaller the resulting heat exchange on the mirror surfaces and its variation with time, the easier the construction of the thermal control system. In this sense, the thermal control system design is double-stage and includes the problem of preliminary temperature stabilization of the spacecraft front assembly. The discussion in this Note demonstrates one possible approach to maintaining a stable front assembly temperature.

Front Assembly Thermostabilization

The problem of the front assembly thermostabilization is studied for a two-mirror telescope shown in Fig. 1. To compare the alternative designs, the concept of the front assembly effective temperature with respect to the primary mirror is introduced by

$$T_{\text{eff}}^4 = F_{m-a} \cdot T_a^4 + \sum_{i=1}^{M} F_{m-i} \cdot T_i^4 \qquad (1)$$

where F_{m-i} is the view factor between the mirror and the black ith surface element of the front assembly, and F_{m-a} takes into account the influence of the front assembly cold aperture with temperature $T_a = 4$ K. The values of T_i are a result of the numerical solution of a radiation heat transfer problem applied to the front assembly, and M is the number of nodes.

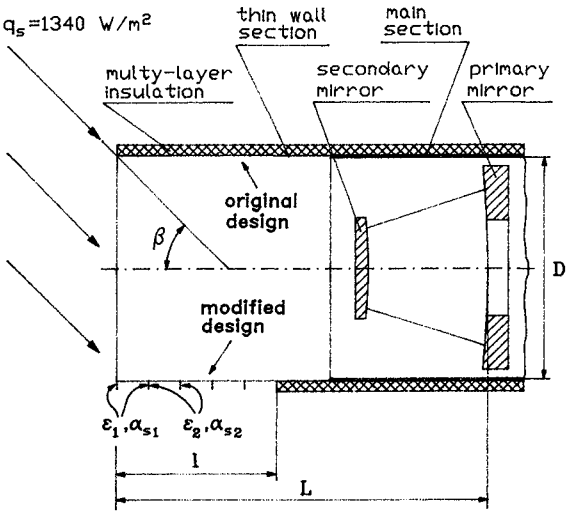

Fig. 1 Front assembly of the space telescope.

For orbits with a variable sun angle β, the value of T_{eff} varies over a wide range. If the telescope thermal control system uses electric heaters, then favorable conditions for its operation will be provided when the value of T_{eff} is slightly lower than the required mirror temperature T_m for all values of β. The extreme ranges of β near 0 and 180 deg may be excluded, because the mirror temperature will not fall outside the tolerable range ($T_{m,\min}$, $T_{m,\max}$) due to its own thermal inertia. In addition, time fluctuations of T_{eff} should be minimized.

The solution of the formulated problem can be achieved, if the total absorption of the solar radiation is uniform in time. In Fig. 1 a possible modification of the front assembly is shown. As compared with the original design, this modification has partial insulation of the exterior surface of the front assembly by multilayer insulation (MLI). The thin ribs are arranged on the exposed exterior surface and have coatings with different values of the solar absorptance α_s and emittance ε, as shown in Fig. 1. This design attempts to equalize the total absorbed solar radiation over a wide range of β.

Plane Ribbed Surface

To perform the preliminary analysis, the exterior cylindrical ribbed surface is described by effective values of $\alpha_{s,\text{eff}}(\beta)$ and ε_{eff}, which are obtained from the simplified plane model (Fig. 2a). The expression for $\alpha_{s,\text{eff}}(\beta)$ is

$$\alpha_{s,\text{eff}}(\beta) = \frac{b|\cos\beta|}{b|\cos\beta| + N \cdot a \cdot \sin\beta}\,\alpha_s + \frac{N \cdot a \cdot \sin\beta}{b|\cos\beta| + N \cdot a \cdot \sin\beta}\,\alpha'_{s,\text{eff}}(\beta) \qquad (2)$$

Received Dec. 6, 1993; revision received March 14, 1994; accepted for publication Nov. 8, 1994.

*Senior Research Scientist, P.O. Box 117.
†Research Scientist, P.O. Box 117.

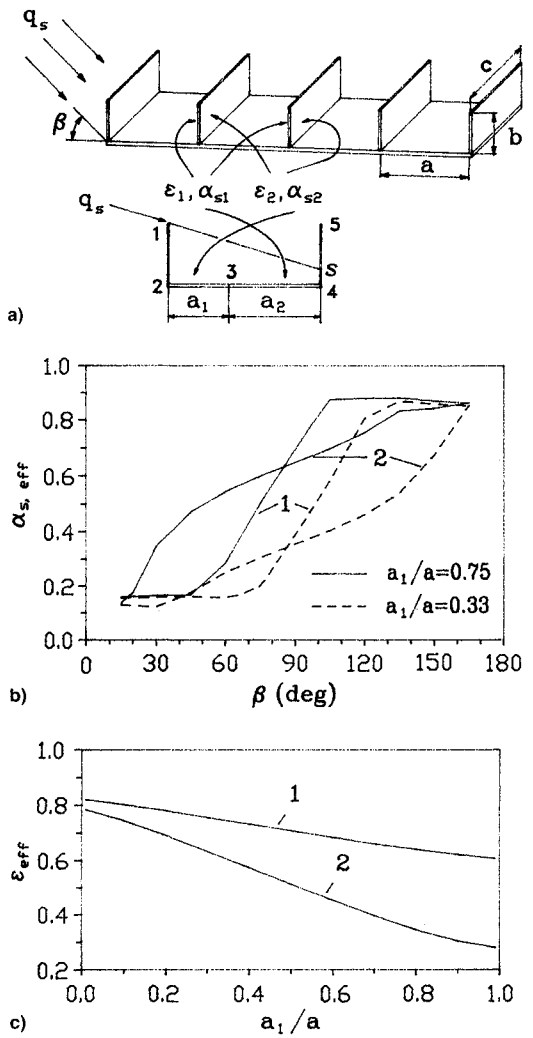

Fig. 2 Ribbed plane surface and its radiative properties: a) geometry, b) $\alpha_{s,eff}$ as a function of sun angle, and c) ε_{eff} as a function of a_1/a. 1, b/a = 1 and 2, b/a = 0.25.

where

$$\alpha_s = \begin{cases} \alpha_{s1}, & 0 \text{ deg} < \beta < 90 \text{ deg} \\ \alpha_{s2}, & 90 \text{ deg} < \beta < 180 \text{ deg} \end{cases} \tag{3}$$

The first term in Eq. (2) describes the absorption on the exterior surfaces of the extreme ribs, and the last term is the absorption in the cells with an effective coefficient $\alpha'_{s,eff}$. If the cell number N is sufficiently large, and the extreme ranges of β are excluded, then the second term dominates and $\alpha_{s,eff} = \alpha'_{s,eff}$. It is not necessary to take into account the extreme values of β near 0 and 180 deg, because, for the first one, additional sunshade protection is necessary, and, for the second one, the front assembly is shielded by the spacecraft. For the extreme values of β, the adopted general thermal model must be modified.

When calculating $\alpha'_{s,eff}$ and ε_{eff}, all surfaces of the cell are assumed to be at the same temperature and all radiative properties are uniform over each area of the cell. These assumptions allow the net-radiation method to be used for radiation flux calculations.[5] All surfaces are opaque and diffusely emitting and reflecting. The calculations assume infinite depth c for each cell and are performed for the two-dimensional cell geometry shown in Fig. 2a. For each value of β, the shadowing area for the cell is calculated and the position of the boundary point s between irradiated and shadowed areas is determined. The points 1–5 with fixed position and the point s with a variable position determine a set of finite size surfaces of the cell thermal model for each value of β. The value of $\alpha'_{s,eff}$ is determined as the ratio of the total absorbed solar radiation in the cell to the incident solar radiation. The value of ε_{eff} is the ratio of the cell-emitted radiation to the blackbody radiation of the plane surface of length a.

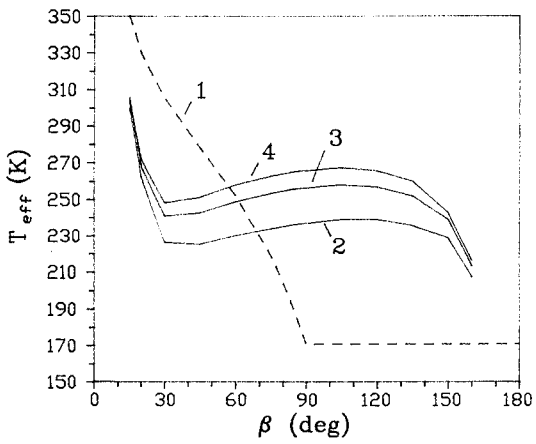

Fig. 3 Effective temperature of the front assembly as a function of sun angle. 1, the entire exterior surface is covered by MLI; 2, 3, 4, modified design: 2, a_1/a = 0.5, 3, a_1/a = 0.67, 4, a_1/a = 0.75.

Two types of thin films are considered for the coatings. The first one has a high solar reflectance (α_{s1} = 0.11, ε_1 = 0.78), and the second one is an absorber of solar radiation (α_{s2} = 0.8, ε_2 = 0.1). The influence of the cell dimensions on $\alpha_{s,eff}(\beta)$ for the chosen coatings is shown in Fig. 2b. The relation b/a determines the curvature of the function $\alpha_{s,eff}(\beta)$, and the value of a_1/a influences its displacement. Combining these parameters, almost any function $\alpha_{s,eff}(\beta)$ with a smooth transition from α_{s1} for $\beta \to 0$ deg to α_{s2} for $\beta \to 180$ deg may be obtained. The effective emittance ε_{eff} (Fig. 2c) does not display an angular dependence for the assumed physical model of the cell. Thus, the plane ribbed surface offers wide opportunities for the control of the function $\alpha_{s,eff}(\beta)$ and the relation $\alpha_{s,eff}/\varepsilon_{eff}$.

Results of Calculations

The preliminary temperature stabilization problem was studied with regard to the primary mirror for the telescope shown in Fig. 1. The effective properties $\alpha_{s,eff}(\beta)$ and ε_{eff} obtained for the plane model were imposed on the exterior cylindrical wall. The calculations of T_{eff} as a succession of steady positions for fixed values of β were performed for the front assembly with L/D = 4 using $M \approx 500$. In addition, the mirror temperature was assumed equal to 290 K.

The results of the calculations are given in Fig. 3. Curve 1 reflects the temperature variation for the original design. The exterior surface ribbing with the cited values of α_s and ε for the thin film coatings, and with b/a = 0.25, L/D = 2 (curves 2, 3, and 4) produces a decrease in the temperature variation with β. As compared with curve 1, within a range of β between 30–100 deg, a reverse tendency in the T_{eff} variation may be obtained.

The cited values of the geometrical parameters and radiative properties are not claimed to be the optimal ones. Their ultimate selection should be based on the complete model, which takes into account the spacecraft configuration and the flight trajectory.

Conclusions

During on-orbit operation, when the sun angle β is a variable, the telescope is affected by variable external conditions that are characterized by the effective temperature T_{eff} of the front assembly. Slight modification of the front assembly con-

struction, based on the exterior surface ribbing, yields a reduction in the variation of T_{eff} and provides for a control of the mean value of T_{eff}. It is possible to apply inclined ribs and ribs of different heights to provide a redistribution of the absorbed solar radiation on the exposed exterior surface.

The advantages of the considered modification decline for β near 0 and 180 deg. However, when the spacecraft operates on the orbit, the effect of external conditions is diminished due to the thermal inertia of the telescope. Therefore, more strict requirements should not be specified to obtain uniformity of the effective temperature.

References

[1]Mason, P. V., "Long-Term Performance of the Passive Thermal Control Systems of the IRAS Spacecraft," *Cryogenics*, Vol. 28, No. 2, 1988, pp. 137–141.

[2]Youdale, J., "State of the Art of ISO," *Cryogenics*, Vol. 29, No. 5, 1989, pp. 528–534.

[3]Murakami, M., Okuda, H., Matsumoto, T., Fujii, G., and Kyoya, M., "Design of Cryogenic System for IRTS," *Cryogenics*, Vol. 29, No. 5, 1989, pp. 553–558.

[4]Akau, R. L., and Larson, D. W., "Thermal Control of Space X-Ray Experiment," *Journal of Spacecraft and Rockets*, Vol. 26, No. 5, 1989, pp. 297–302.

[5]Siegel, R., and Howell, J. R., "Thermal Radiation Heat Transfer," McGraw–Hill, New York, 1972.

Study of Transpiration Cooling over a Flat Plate at Hypersonic Mach Numbers

Sreekanth* and N. M. Reddy†
Indian Institute of Science, Bangalore 560 012, India

Nomenclature

C_h = Stanton number
E = relative change
h = enthalpy
k = thermal conductivity
M = Mach number
$\dot{m}$ = mass injection rate
$\dot{q}$ = heat flux
Re = Reynolds number
T = temperature
x = distance along the plate measured from the leading edge
y = distance normal to the surface (also y coordinate)

Subscripts
a = aerodynamic
C = coolant
r = recovery
W = wall
∞ = freestream

Superscripts
$*$ = dimensional quantities
est = estimated value

Received April 22, 1994; presented as Paper 94-2075 at the AIAA/ASME Joint Thermophysics and Heat Transfer Conference, Colorado Springs, CO, June 20–23, 1994; revision received Nov. 16, 1994; accepted for publication Dec. 12, 1994.

*Research Scholar, Department of Aerospace Engineering; currently Engineer of VSSC.

†Professor, Department of Aerospace Engineering. Associate Fellow AIAA.

Introduction

AERODYNAMIC heating is a major concern in the design of hypersonic transport vehicles. Although various cooling systems have been adopted in the past to protect the vehicle from excessive heating, their usage with respect to the concept of hypersonic transport is doubtful. Hence, alternative forms of cooling systems have to be evolved. A comparative study of various cooling systems made by McConarty and Anthony[1] indicated that the transpiration cooling system, on which the present study is focused, has the potential to cool the hypersonic cruise vehicles effectively. Although the literature on this subject is very rich, most of the theoretical work done was based on approximate equations such as boundary-layer and viscous shock-layer equations. Apart from this, many of these analyses were restricted to a particular region in the flowfield, such as the stagnation point. These analyses, in spite of the approximations involved at various levels, have given very good physical insight into the subject. Nevertheless, owing to the approximations made in these analyses, their results will have limited applications. Often it is difficult to say whether the solutions obtained through these analyses are unique or not,[2] unless a less approximate analysis confirms it. Moreover, for cases where flow separation occurs or a shock–shock or shock–boundary-layer interaction occurs, such an analysis cannot be made. In essence, there is an overall need for making a more accurate study of transpiration cooling. Recently, Sreekanth and Reddy[3] made a study based on Navier–Stokes equations. This Note is a short version of Ref. 3.

Problem Statement

The objective of the present work is to perform transpiration cooling analysis using Navier–Stokes equations. Also, unlike the earlier studies, the present work does not assume an isothermal wall with a prescribed wall temperature. Instead, the temperature of the coolant in the storage T_C^* is prescribed and the wall temperature T_W^* is obtained as a solution for this coolant temperature. In the authors' opinion this situation mimics the actual situation more realistically than the earlier studies.

The transpiration cooling mechanism can be classified into two phases. In the first phase (preinjection phase), the coolant temperature is raised from its storage value T_C^* to the value at the surface T_W^* by absorbing some of the oncoming heat. In the second phase (postinjection phase), the injected gas mixes with boundary-layer gas and partially blocks the heat transfer to the surface itself. In the present work, the wall temperature is calculated assuming that the coolant absorbs all the heat coming into the surface in the preinjection phase of cooling. Under such conditions, the heat balance at the surface leads to $\dot{q}_a^* = -\dot{q}_C^*$, where $\dot{q}_a^*$ is the aerodynamic heat load and $\dot{q}_C^*$ is the heat gained by the coolant before injection. By using appropriate expressions for $\dot{q}_a^*$ and $\dot{q}_C^*$ we get

$$k^* \frac{\partial T^*}{\partial y^*} = \dot{m}_W^*(h_W^* - h_C^*) \tag{1}$$

Eq. (1) is written in dimensional form. It should be noted that in the absence of gas injection, Eq. (1) leads to adiabatic wall condition. In this Note, the situation represented by Eq. (1) is referred to as the "no net heat flow into the wall" condition. Transpiration cooling analysis has been made for